Published in final edited form as:

Brain Behav Immun. 2018 February ; 68: 98–110. doi:10.1016/j.bbi.2017.10.005.

Impact of peripheral immune status on central molecular responses to facial nerve axotomy

Deborah O. Setter[1,2], **Elizabeth M. Runge**[1,2], **Nicole D. Schartz**[1], **Felicia M. Kennedy**[1,2], **Brandon L. Brown**[1], **Kathryn P. McMillan**[1,2], **Whitney M. Miller**[1,2], **Kishan M. Shah**[1], **Melissa M. Haulcomb**[1,2], **Virginia M. Sanders**[3], and **Karthryn J. Jones**[1,2]

[1]Department of Anatomy and Cell Biology, Indiana University School of Medicine, Indianapolis, IN

[2]Research and Development Service, Richard L. Roudebush VAMC, Indianapolis, IN

[3]Molecular Virology, Immunology, and Medical Genetics, The Ohio State University, Columbus, OH

Abstract

When facial nerve axotomy (FNA) is performed on immunodeficient recombinase activating gene-2 knockout (RAG-2$^{-/-}$) mice, there is greater facial motoneuron (FMN) death relative to wild type (WT) mice. Reconstituting RAG-2$^{-/-}$ mice with whole splenocytes rescues FMN survival after FNA, and CD4+ T cells specifically drive immune-mediated neuroprotection. Evidence suggests that immunodysregulation may contribute to motoneuron death in amyotrophic lateral sclerosis (ALS). Immunoreconstitution of RAG-2$^{-/-}$ mice with lymphocytes from the mutant superoxide dismutase (mSOD1) mouse model of ALS revealed that the mSOD1 whole splenocyte environment suppresses mSOD1 CD4+ T cell-mediated neuroprotection after FNA. The objective of the current study was to characterize the effect of CD4+ T cells on the central molecular response to FNA and then identify if mSOD1 whole splenocytes blocked these regulatory pathways.

Gene expression profiles of the axotomized facial motor nucleus were assessed from RAG-2$^{-/-}$ mice immunoreconstituted with either CD4+ T cells or whole splenocytes from WT or mSOD1 donors. The findings indicate that immunodeficient mice have suppressed glial activation after axotomy, and cell transfer of WT CD4+ T cells rescues microenvironment responses. Additionally, mSOD1 whole splenocyte recipients exhibit an increased astrocyte activation response to FNA. In RAG-2$^{-/-}$ + mSOD1 whole splenocyte mice, an elevation of motoneuron-specific Fas cell death pathways is also observed. Altogether, these findings suggest that mSOD1 whole splenocytes do not suppress mSOD1 CD4+ T cell regulation of the microenvironment, and instead, mSOD1 whole splenocytes may promote motoneuron death by either promoting a neurotoxic astrocyte phenotype or inducing Fas-mediated cell death pathways. This study demonstrates that peripheral immune status significantly affects central responses to nerve injury. Future studies will elucidate

Corresponding Author: Deborah Setter dolmstea@iupui.edu, 320 W 15th St. NB211C, Indianapolis, IN 46202.

the mechanisms by which mSOD1 whole splenocytes promote cell death and if inhibiting this mechanism can preserve motoneuron survival in injury and disease.

Keywords

Motoneuron; nerve injury; axotomy; T cells; amyotrophic lateral sclerosis

1. Introduction

A growing body of literature indicates that peripheral immune status is an important factor in central nervous system responses to injury or disease (Beers et al., 2008; DeFrancesco-Lisowitz et al., 2015; Ip et al., 2015; Spani et al., 2015). Using the facial nerve axotomy (FNA) model of peripheral nerve injury, our laboratory discovered that immunodeficient mice lacking functional B and T cells have significantly more facial motoneuron (FMN) death within the central nervous system (CNS) after FNA relative to wild type (WT) mice (Serpe et al., 1999; Serpe et al., 2000; Serpe et al., 2003). Immunoreconstitution of immunodeficient mice with WT whole splenocytes prior to FNA rescues FMN survival, and the CD4+ T cell population alone is specifically responsible for mediating neuroprotection after axotomy (Serpe et al., 2003). Key cellular elements within the facial motor nucleus that interact with peripheral neuroprotective CD4+ T cells include both astrocytes and microglia (Byram et al., 2004; Wainwright et al., 2009b; Wainwright et al., 2009c).

CD4+ T cells are implicated in amyotrophic lateral sclerosis (ALS), a neurodegenerative disease affecting motoneurons. CD4+ T cells are decreased in ALS patients relative to age-matched controls (Chen et al., 2014), and patients with ALS exhibit increased peripheral immune activation and circulating cytokines (Chen et al., 2014; Lu et al., 2016). The mutant superoxide dismutase (mSOD1) mouse model of ALS also demonstrates significant immunodysregulation, including lymphopenia and a failure of T cells to generate a proliferation or immunization response to stimuli (Kuzmenok et al., 2006; Banerjee et al., 2008). CD4+ T cell deficiency in mSOD1 mice results in accelerated disease progression, and adoptive cell transfer of WT CD4+ T cells into mSOD1 mice modestly improves survival (Banerjee et al., 2008; Beers et al., 2008). Thus, the immune system may be a new therapeutic target for ALS.

When FNA is superimposed on the mSOD1 mouse in the pre-symptomatic stages, FMN death after FNA mirrors that of immunodeficient mice, corroborating evidence for immunodysregulation in mSOD1 mice (Mariotti et al., 2002; Mesnard et al., 2011). These intriguing findings led us to explore the molecular changes that occur in the facial motor nucleus of both FMN and the surrounding neuropil in WT and mSOD1 mice (Mesnard et al., 2011; Haulcomb et al., 2014). Genes associated with MN regeneration, glial activation, inflammation, and cell death were examined. While the FMN regenerative phenotype in mSOD1 mice was unaffected, astrocyte and microglia responses were found to be dysregulated by peripheral axotomy in mSOD1 mice. Furthermore, mSOD1 mice also exhibited increased expression of motoneuron-specific Fas cell death pathway components, indicating a disease-induced prevalence of Fas-mediated cell death (Haulcomb et al., 2014).

We next explored the neuroprotective capacity of the mSOD1 peripheral immune system in immunodeficient mice. When whole splenocytes from mSOD1 mice, including CD4+ T cells, were transferred into RAG-2$^{-/-}$ mice, significant FMN death still occurred after FNA. However, when isolated mSOD1 CD4+ T cells were transferred into RAG-2$^{-/-}$ mice, we observed that FMN survival was rescued to WT levels (Mesnard-Hoaglin et al., 2014). These findings suggest that an inhibitory factor present in the mSOD1 whole splenocyte milieu blocks mSOD1 CD4+ T cell-mediated neuroprotection.

While we now have an understanding of the cellular elements involved in CD4+ T cell-mediated prevention of FMN loss after target disconnection, the accompanying key molecular changes that occur in the CNS, and how they may factor in ALS, are unknown. The well-characterized nerve cell body response to injury in the facial nucleus provides the opportunity to exploit the advantages inherent in laser microdissection and qPCR in order to identify a CNS molecular signature modifiable by the peripheral immune system after injury (Lieberman, 1971; Grafstein, 1975; Moran & Graeber, 2004). This approach is both powerful and efficient because it captures large amounts of gene expression data reflecting different functional states and multiple cell types using a single method of tissue processing from individual animals.

The results indicate that the CNS astrocytic response to peripheral nerve injury appears to be differentially affected by peripheral immune status. Furthermore, mSOD1 immune cells induce Fas expression in the facial motor nucleus, which may contribute to motoneuron death. Collectively, these data suggest that cell-cell interactions between the CNS glia and adaptive immune are potential therapeutic targets in neurodegenerative diseases such as ALS.

2. Materials and Methods

2.1. Animals and surgical procedure

For this study, the following mouse strains were purchased from The Jackson Laboratory (Bar Harbor, ME) where they were bred and maintained in separate lines: C57BL/6J (WT, RRID:IMSR_JAX:000664), B6(Cg)-Rag2tm1.1Cgn/J (RAG-2$^{-/-}$, RRID:IMSR_JAX:008449), and B6.Cg-Tg(SOD1G93A)1Gur/J (mSOD1, RRID:IMSR_JAX:004435). WT and RAG-2-/-strains are maintained as homozygous inbred colonies. The mSOD1 strain is maintained by breeding a C57BL/6J female with a male hemizygous for the SOD1G93A mutation. All mice were obtained at 6 or 7 weeks of age and allowed to acclimate for 1 week prior to any manipulation. Female mice were exclusively used, which is a limitation of this study. Male mice were excluded because their propensity for aggression after surgery requires individual housing to prevent trauma and infection of the surgical site (Edwards, 1968; Van Loo et al., 2003; Lockworth et al., 2015). Individual housing significantly stresses the animal, resulting in adverse effects on both immune physiology and animal welfare (Olsson & Westlund, 2007; Kamakura et al., 2016; Weber et al., 2017).

All animal procedures complied with National Institutes of Health guidelines on the care and use of laboratory animals and were approved by Indiana University School of Medicine's Institutional Animal Care and Use Committee. Mice were housed in sterilized microisolater

cages with a 12 hr light/dark cycle and fed autoclaved food pellets and drinking water *ad libitum*. The animal facility uses a laminar flow system to maintain a pathogen-free environment.

Aseptic procedures were followed during the FNA following National Institute of Health guidelines. FNA was performed on 8 week old mice following previously established methods (Olmstead et al., 2015). Briefly, mice were anesthetized with 2.5% isoflurane in 0.9 L/min oxygen, and the facial nerve was exposed and transected at its exit from the stylomastoid foramen. The remaining nerve stumps were separated and resected to prevent reconnection. No operation was performed on the left facial nerve, allowing for the left facial motor nucleus to serve as a paired internal control. Prior to euthanasia, behavioral observations of ipsilateral facial paralysis verified that no functional recovery occurred.

2.2. Isolation and adoptive transfer of whole splenocytes and CD4+ T cells

Adoptive cell transfers were performed on recipient mice at 7 weeks of age, 1 week prior to FNA following a protocol modified from Serpe et al., 2003. Donor mice (1:1 donor:recipient ratio) were euthanized with CO_2 inhalation followed by cervical dislocation. The spleen was dissected out and a single-cell suspension of whole splenocytes was generated following the Miltenyi Biotec gentleMACS protocol.

For preparation of whole splenocytes, red blood cell lysis was performed on the cell suspension with ACK Lysing Buffer (Thermo Fisher Scientific; A1049201) for 4 min at RT, and cells were washed and resuspended in PBS. 50×10^6 whole splenocytes in 100 μl of PBS were injected into the recipient mouse tail vein.

For preparation of CD4+ T cells, red blood cell lysis was not performed to maximize CD4+ T cell yield. The whole splenocyte cell pellet was incubated with CD4 (L3T4) MicroBeads (Miltenyi Biotec, 130-049-201) per manufacturer protocol, and magnetic separation was performed with the Possel_d2 program on an autoMACS™ Pro Separator. Cells were washed and resuspended in PBS, and 5×10^6 CD4+ T cells in 100 μl of PBS were injected into the recipient mouse tail vein. This cell number was selected based on data indicating that approximately 10% of whole splenocytes are CD4+ T cells in the C57BL/6J mouse strain (Laboratory).

CD4+ T cell fraction purity was measured using flow cytometry with FITC rat anti-mouse CD4 antibody (BD Biosciences Cat# 557307 RRID:AB_396633), and average purity levels were greater than 90% in accordance with previously published work from our laboratory (Serpe et al., 2003).

2.3. Laser capture microdissection

Experimental animals (n = 6-12/timepoint/group) were euthanized via CO_2 inhalation followed by cervical dislocation at 7, 14, 28, and 56 days post-operation (dpo). An unoperated group was also included as a 0 dpo control. Brains were rapidly removed and immediately flash frozen, as described previously (Mesnard et al., 2010). 25 μm cryostat sections of the entire rostral-caudal extent of the facial nucleus within the brainstem were collected on Leica glass polyethylene foil membrane slides (Nuhsbaum, McHenry, IL,

11505158). Tissue staining and laser capture microdissection were performed using methods previously described (Mesnard et al., 2010). The right (axotomized, Ax) and left (control, C) facial motor nuclei were laser captured using a Leica ASLMD.

2.4. RNA extraction and reverse transcription

RNA extraction was performed per the Arcturus PicoPure® RNA Isolation Kit protocol (Thermo Fisher Scientific; KIT0204). RNA yield was quantified with a NanoDrop 2000 Spectrophotometer. 60 ng of RNA was reverse transcribed into cDNA using the SuperScript® VILO cDNA Synthesis Kit and Master Mix following manufacturer instructions (Thermo Fisher Scientific; 11754050).

2.5. qPCR

qPCR was performed using an Eppendorf Realplex Mastercycler system. The 20 μl reaction volume contained 1 μl of cDNA, 1 μl of 20× TaqMan® FAM gene expression assay (Table 1), 8 μl of 0.002% diethyl pyrocarbonate-treated water, and 10 μl of TaqMan Gene Expression Master Mix (Thermo Fisher Scientific; 4369016). The qPCR program was as follows: UDG optimization at 50°C for 2 min, AmpliTaq Gold Activation at 95°C for 10 min, and 40 cycles of denaturation at 95°C for 15 sec followed by annealing/extension at 60°C for 1 min.

We have previously established percent-changes in mRNA expression after axotomy using custom-made primers and SYBR® green reagents (Mesnard et al., 2010; Mesnard et al., 2011; Haulcomb et al., 2014). We opted to use TaqMan assays in this study because of their enhanced sensitivity and specificity for gene targets (Alvarez & Done, 2014). To validate use of TaqMan assays, side-by-side comparisons of results were obtained using the SYBR and TaqMan systems. This comparison revealed that both SYBR and TaqMan yielded similar results for all genes of interest except *Cd68* and *Tnfr1* (data not shown). To maintain consistency with previously established results, custom primers and TaqMan probes were used for *Cd68* (F 5′-CCCAAATTCAAATCCGAATCC-3′, R 5′-GGTACCGTCACAACCTCC-3′, probe 5′-AAAGTGAGTGCGTCCCTTGCAGCC-3′) and *Tnfr1* (F 5′-TGCCATGCAGGGTTCTTTCTG-3′, R 5′-TTTGCAAGCGGAGGAGGTAGG-3′, probe 5′-ACCCAATTCAGGGTGGAAGAAAGGT-3′).

2.6. Statistical analysis of qPCR data

The percent change in mRNA expression between axotomized and control facial motor nuclei was calculated using the Pfaffl method, with glyceraldehyde 3-phosphate dehydrogenase (*Gapdh*) as the reference gene (Pfaffl, 2001). Relative gene expression of *Tnfα* compared to *Gapdh* was used to quantify mRNA expression in the axotomized facial motor nucleus because there was no detectable expression of *Tnfα* in the control facial motor nucleus. The Grubbs' test was performed on the calculated values to detect and remove outliers (GraphPad QuickCalcs, www.graphpad.com, RRID:SCR_000306). Statistical significance was calculated using two-way ANOVA (factors: group × postoperative time, for each individual gene) followed by Student-Neuman-Keuls post hoc

multiple comparisons analysis with a significance level of $p < 0.05$ in SigmaPlot (SigmaPlot, version 13.0, https://systatsoftware.com/products/sigmaplot/, RRID:SCR_003210).

To validate that axotomy does not induce mRNA expression changes in the control facial motor nucleus, one-way ANOVA of the relative expression of each gene of interest compared to GAPDH within the control facial motor nucleus was performed at each postoperative timepoint with $p < 0.05$. For all genes examined, no statistically significant changes were detected (data not shown).

3. Results

3.1. Axotomy-induced pro-regeneration gene expression in WT, immunodeficient and WT CD4+ T cell immunoreconstituted facial motor nuclei

Axotomy-induced expression of β_{II}-tubulin and growth-associated protein 43 (Gap-43) mRNA and protein by motoneurons is key to successful axonal elongation and target reconnection (Tetzlaff et al., 1991; Armstrong et al., 2008). These gene expression changes occur even when the axon is physically prevented from reconnecting to target, as is the case in this study (Mesnard et al., 2010).

Analysis of *β_{II}-tubulin* mRNA expression in the experimental groups revealed that both group and postoperative time had significant effects ($F_{2,75} = 4.07$, $p = 0.021$; $F_{4,75} = 68.98$, $p < 0.001$, respectively). In the WT group, expression of *β_{II}-tubulin* was significantly increased relative to unoperated controls at 7, 14, and 28 dpo (163 ± 12%, 168 ± 19%, and 57 ± 15%, respectively; $p < 0.05$), and levels returned to baseline at 56 dpo. In the RAG-2$^{-/-}$ group, *β_{II}-tubulin* expression was significantly elevated relative to unoperated controls at 7 and 14 dpo (160 ± 21% and 178 ± 19%, respectively; $p < 0.05$), and expression was not different compared to baseline levels at 28 and 56 dpo. In the RAG-2$^{-/-}$ group with adoptive transfer of WT CD4+ T cells, *β_{II}-tubulin* expression was significantly higher relative to unoperated controls at 7, 14, and 28 dpo (169 ± 13%, 171 ± 14%, and 96 ± 14%, respectively; $p < 0.05$), and expression reverted to uninjured levels at 56 dpo. No statistically significant differences were detected in the *β_{II}-tubulin* gene expression response between WT and RAG-2$^{-/-}$ groups nor between WT and RAG-2$^{-/-}$ + WT CD4+ T cells groups. There was significantly higher *β_{II}-tubulin* expression levels in RAG-2$^{-/-}$ + WT CD4+ mice compared to RAG-2$^{-/-}$ mice at 28 dpo ($p = 0.026$; Fig. 1A).

Comparison of *Gap-43* mRNA expression in the experimental groups revealed that both group and postoperative time had significant effects ($F_{2,80} = 10.48$, $p < 0.001$; $F_{4,80} = 161.18$, $p < 0.001$, respectively). In the WT group, expression of *Gap-43* was significantly increased compared to unoperated controls at 7, 14, and 28 dpo (1083 ± 41%, 1239 ± 128%, and 351 ± 38%, respectively; $p < 0.05$), and expression returned to baseline levels at 56 dpo. In the RAG-2$^{-/-}$ group, *Gap-43* expression was significantly elevated relative to unoperated controls at 7 and 14 dpo (873 ± 77% and 1057 ± 79%, respectively; $p < 0.05$), and expression was not different compared to baseline at 28 and 56 dpo. In the RAG-2$^{-/-}$ group with adoptive transfer of WT CD4+ T cells, *Gap-43* expression was significantly higher relative to unoperated controls at 7, 14, and 28 dpo (1342 ± 81%, 1286 ± 92%, and 495 ± 79%, respectively; $p < 0.05$) and no different from control at 56 dpo. There were no

statistically significant differences in post-axotomy *Gap-43* expression responses between WT and RAG-2$^{-/-}$ groups. The RAG-2$^{-/-}$ + WT CD4+ T cells group had a significant increase in *Gap-43* expression relative to WT at 7 dpo ($p = 0.038$). The RAG-2$^{-/-}$ + WT CD4+ T cells group also had a statistically significant increase in *Gap-43* expression compared to the RAG-2$^{-/-}$ group at 7, 14, and 28 dpo ($p < 0.001$, 0.020, and 0.004, respectively; Fig. 1B)

In summary, immunodeficiency does not affect the regenerative response of the axotomized FMN, and adoptive transfer of WT CD4+ T cells results in a modest increase in activation of the motoneuron regenerative program.

3.2. Axotomy-induced glial gene expression in WT, immunodeficient, and WT CD4+ T cell immunoreconstituted facial motor nuclei

Astrocytes and microglia play a key role after facial nerve injury, and their response to FNA has been well documented (Graeber et al., 1988; Tetzlaff et al., 1988). Astrocytes upregulate expression of glial fibrillary acidic protein (GFAP), a cytoskeletal protein, and microglia upregulate cluster of differentiation 68 (CD68), a lysosomal protein, as they respond to the FNA.

Examining *Gfap* mRNA expression in the experimental groups revealed that both group and postoperative time had significant effects ($F_{2,76} = 9.88$, $p < 0.001$; $F_{4,76} = 47.09$, $p < 0.001$, respectively), and there was significant interaction in group × postoperative time ($F_{8,76} = 3.56$, $p = 0.001$). In the WT group, expression of *Gfap* was significantly increased relative to unoperated controls at 7, 14, 28, and 56 dpo (909 ± 97%, 805 ± 71%, 644 ± 121%, and 306 ± 45%, respectively; $p < 0.05$). In the RAG-2$^{-/-}$ group, *Gfap* expression was significantly elevated relative to unoperated controls at 7 and 14 dpo (782 ± 249% and 480 ± 79%, respectively; $p < 0.05$), and expression prematurely returned to baseline levels at 28 and 56 dpo. In the RAG-2$^{-/-}$group with adoptive transfer of WT CD4+ T cells, *Gfap* expression was significantly higher relative to unoperated controls at 7, 14, 28, and 56 dpo (646 ± 32%, 911 ± 31%, 763 ± 97%, and 236 ± 79, respectively; $p < 0.05$). There were statistically significant decreases in *Gfap* expression in the RAG-2$^{-/-}$ group relative to WT and RAG-2$^{-/-}$ + WT CD4+ T cells groups at 14 and 28 dpo (vs. WT: $p = 0.029$, 0.003, respectively; vs. RAG-2$^{-/-}$ + WT CD4+ T cells: $p < 0.001$ at both timepoints). There were no statistically significant differences between the WT and RAG-2$^{-/-}$ + WT CD4+ T cell groups (Fig. 2A).

Comparison of *Cd68* mRNA expression in the experimental groups revealed that both group and postoperative time had significant effects ($F_{2,87} = 4.94$, $p = 0.009$; $F_{4,87} = 28.66$, $p < 0.001$, respectively). In the WT group, expression of *Cd68* was significantly increased compared to unoperated controls at 7, 14, and 28 dpo (823 ± 109%, 772 ± 117%, 664 ± 78%, respectively; $p < 0.05$), and expression returned to baseline levels at 56 dpo. In the RAG-2$^{-/-}$ group, *Cd68* expression was significantly elevated relative to unoperated controls at 7 and 14 dpo (541 ± 73%, 654 ± 28%, respectively; $p < 0.05$), and expression reverted to baseline levels at 28 and 56 dpo. In the RAG-2$^{-/-}$ group with adoptive transfer of WT CD4+ T cells, *Cd68* expression was significantly higher relative to unoperated controls at 7, 14, 28, and 56 dpo (749 ± 93%, 810 ± 62%, 626 ± 104%, and 363 ± 103%, respectively; $p < 0.05$). There was a statistically significant decrease in *Cd68* expression in the RAG-2$^{-/-}$ group

relative to WT at 28 dpo ($p = 0.036$). In addition, there were significantly decreased *Cd68* levels in the RAG-$2^{-/-}$ group relative to the RAG-$2^{-/-}$ + WT CD4+ T cells group at 28 and 56 dpo ($p = 0.011$ and 0.037, respectively). There were no statistically significant differences between WT and RAG-$2^{-/-}$ + WT CD4+ T cells groups at any of the timepoints examined (Fig. 2B).

To further establish that facial nerve axotomy results in reactive glial changes, we performed a supplementary experiment evaluating mRNA changes for another marker of microglial activation, allograft inflammatory factor 1 (*Aif1*, the transcript name for ionized calcium binding adaptor Iba1), which revealed a similar pattern of expression in WT as *Cd68* (Supplemental Results, Fig. S1). We also evaluated GFAP and Iba1 protein expression changes in the WT axotomized facial motor nucleus and observed an increase in immunoreactivity for these markers at a time point corresponding to the peaks of their respective mRNA expression (Supplemental Results, Fig. S2), suggesting that our observed mRNA expression patterns reflect downstream protein changes.

Overall, immunodeficiency results in a significant decrease in both astrocyte and microglia activation responses to FNA, with the astrocyte reaction being more severely affected by immunodeficiency. Adoptive transfer of WT CD4+ T cells restores both astrocyte and microglia activation to WT levels at all post-axotomy timepoints, indicating that WT CD4+ T cells are key regulators of the glial response to FNA.

3.3. Axotomy-induced Tnf axis gene expression in WT, immunodeficient and WT CD4+ T cell immunoreconstituted facial motor nuclei

Tnfα is a proinflammatory cytokine that is necessary for microglia expression of αXβ2 integrin, MHC I, and B7.2 costimulatory molecule expression after facial nerve injury (Raivich, 2002; Bohatschek et al., 2004a; Bohatschek et al., 2004b). Additionally, knocking out both TNFR1&2 simultaneously promotes motoneuron survival after facial nerve injury, suggesting that TNFα may have dual roles in immune-mediated neuroprotection (Raivich, 2002). TNFR1 is a receptor that trimerizes after binding to TNFα and can either induce apoptosis via caspase 8 or trigger inflammatory gene expression via AP-1 and NF-κB (Baud & Karin, 2001; Wajant & Scheurich, 2011). Because of its association with cell death pathways, *Tnfα* and *Tnfr1* expression were analyzed as possible contributors to the increased FMN death observed in RAG-$2^{-/-}$ mice. In addition, *Tnfα* served as a marker for the inflammatory status of the post-axotomy facial motor nucleus.

For all groups and timepoints, there was no detectable *Tnfα* expression in the control facial motor nucleus. Therefore, data shown is relative gene expression from the axotomized side only. Analysis of *Tnfα* mRNA expression in the experimental groups revealed that both group and postoperative time had significant effects ($F_{2,74} = 19.78$, $p < 0.001$; $F_{4,74} = 18.12$, $p < 0.001$, respectively), and there was significant interaction in group × postoperative time ($F_{8,74} = 4.44$, $p < 0.001$). In the WT group, *Tnfα* expression was significantly increased relative to unoperated controls at 7 and 14 dpo (4.4 ± 0.9 and 2.7 ± 1.0, respectively; $p < 0.05$), and expression returned to baseline levels at 28 and 56 dpo. In the RAG-$2^{-/-}$ group, expression of *Tnfα* was not significantly different from unoperated controls at any of the observed timepoints. In the RAG-$2^{-/-}$ group with adoptive transfer of WT CD4+ T cells,

Tnfa expression was significantly higher relative to unoperated controls at 7, 14, and 28 dpo (3.3 ± 0.5, 5.6 ± 1.0, and 3.2 ± 0.7, respectively; $p < 0.05$), and levels reverted to baseline expression at 56 dpo. There were statistically significant decreases in *Tnfa* expression in the RAG-2$^{-/-}$ group relative to both WT and RAG-2$^{-/-}$ + WT CD4+ T cells groups at 7 dpo ($p < 0.001$ for each). In addition, *Tnfa* expression was significantly decreased in the RAG-2$^{-/-}$ group compared to the RAG-2$^{-/-}$ + WT CD4+ T cells group at 14 and 28 dpo ($p < 0.001$ and $p = 0.001$, respectively) There were also statistically significant differences between the WT and RAG-2$^{-/-}$ + WT CD4+ T cell groups at 14 dpo ($p = 0.004$, Fig. 3A).

Comparison of *Tnfr1* mRNA expression in the experimental groups revealed that both group and postoperative time had significant effects ($F_{2,79} = 31.42$, $p < 0.001$; $F_{4,79} = 26.79$, $p < 0.001$, respectively), and there was significant interaction in group × postoperative time ($F_{8,79} = 7.74$, $p < 0.001$). In the WT group, expression of *Tnfr1* was significantly increased compared to unoperated controls at 7 dpo (119 ± 31%, $p < 0.05$), and expression was not different from control at 14, 28, or 56 dpo. In the RAG-2$^{-/-}$ group, *Tnfr1* expression was significantly elevated relative to unoperated controls at 14 dpo (139 ± 29%, $p < 0.05$), and expression was not significantly different from baseline at 7, 28, or 56 dpo. In the RAG-2$^{-/-}$ group with adoptive transfer of WT CD4+ T cells, *Tnfr1* expression was significantly higher relative to unoperated controls at 7, 14, 28, and 56 dpo (219 ± 13%, 220 ± 15%, 135 ± 12%, and 73 ± 6%, respectively; $p < 0.05$). There were significant differences in *Tnfr1* expression in comparing the WT and RAG-2$^{-/-}$ groups at 7 and 14 dpo ($p < 0.001$ and 0.029). In addition, there were statistically significant increased *Tnfr1* levels in the RAG-2$^{-/-}$ + WT CD4+ T cells group compared to both WT and RAG-2$^{-/-}$ groups at 7, 14, and 28 dpo (vs. WT: $p < 0.001$, < 0.001, and 0.005, respectively; vs. RAG-2$^{-/-}$: $p < 0.001$, 0.002, and 0.001, respectively; Fig. 3B).

In summary, there is decreased *Tnfa* expression and a delayed *Tnfr1* response with immunodeficiency, and adoptive transfer of WT CD4+ T cells restores and increases both *Tnfa* and *Tnfr1* expression. These results indicate that the immune system is an important regulator of the TNF axis in the CNS molecular response to FNA.

3.4. Axotomy-induced Fas/nNos cell death signaling pathway gene expression in WT, immunodeficient and WT CD4+ T cell immunoreconstituted facial motor nuclei

Motoneurons from mSOD1 mice are highly vulnerable to cell death via the Fas/neuronal nitric oxide synthase (nNos) cell death cascade (Raoul et al., 2002; Raoul et al., 2006). A study of cell death receptor expression on mSOD1 mice after FNA revealed that Fas/nNos signaling was highly expressed relative to WT, suggesting that the mSOD1 mutation leads to prominent expression of this cell death pathway (Haulcomb et al., 2014). Because Fas/nNos is related to motoneuron death after target disconnection in mSOD1 disease pathology, we wanted to explore if it played a role in the increased FMN death observed in immunodeficient animals.

Analysis of *Fas* mRNA expression in the experimental groups revealed that both group and postoperative time had significant effects ($F_{2,84} = 5.30$, $p = 0.007$; $F_{4,8}4 = 7.93$, $p < 0.001$, respectively). In the WT group, *Fas* expression was significantly increased relative to unoperated controls at 7, 14, 28, and 56 dpo (70 ± 12%, 62 ± 16%, 62 ± 16%, and 63 ± 21%,

respectively; $p < 0.05$). In the RAG-2$^{-/-}$ group, expression of *Fas* was not significantly different from unoperated controls at any of the observed timepoints. In the RAG-2$^{-/-}$ group with adoptive transfer of WT CD4+ T cells, *Fas* expression was not different from baseline at 7 and 14 dpo, and expression was significantly higher relative to unoperated controls at 28 and 56 dpo (76 ± 14% and 84 ± 29%, respectively; $p < 0.05$). There was significantly higher expression of *Fas* in the WT group relative to the RAG-2$^{-/-}$ group at 7 and 14 dpo ($p = 0.002$ and 0.043, respectively). *Fas* expression was also significantly higher in the WT group relative to RAG-2$^{-/-}$ + WT CD4+ T cells at 7 dpo ($p = 0.004$). Increased *Fas* expression was also observed in RAG-2$^{-/-}$ + WT CD4+ T cells compared to RAG-2$^{-/-}$ at 56 dpo ($p = 0.006$; Fig. 4A).

Comparison of *nNos* mRNA expression in the experimental groups revealed that both group and postoperative time had significant effects ($F_{2,76} = 10.51$, $p < 0.001$; $F_{4,76} = 8.17$, $p < 0.001$, respectively). In the WT and RAG-2$^{-/-}$ groups, expression of *nNos* was not significantly different compared to unoperated controls at any of the examined timepoints. In the RAG-2$^{-/-}$group with adoptive transfer of WT CD4+ T cells, *nNos* expression was significantly higher relative to unoperated controls at 56 dpo (92 ± 23%, $p < 0.05$). In comparing WT and RAG-2$^{-/-}$ groups, there was significantly different expression of *nNos* at 28 dpo ($p = 0.042$). The RAG-2$^{-/-}$ + WT CD4+ T cells group has significantly higher *nNos* expression relative to both WT and RAG-2$^{-/-}$ groups at 56 dpo ($p < 0.001$ for both; Fig. 4B).

In summary, there is no evidence that the increased FMN death after FNA in immunodeficient RAG-2$^{-/-}$ mice is due to the Fas/nNos death cascade. Furthermore, WT CD4+ T cells do not significantly alter expression of components of the Fas death pathway except for the increased nNos observed at 56 dpo, a timepoint beyond the 28 dpo timepoint when maximum immune-mediated neuroprotection is observed.

3.5. Axotomy-induced pro-regenerative gene expression in immunodeficient mice with mSOD1 immunoreconstitution

The following set of experiments were designed to examine the differences in gene expression responses to axotomy between RAG-2$^{-/-}$ mice reconstituted with mSOD1 whole splenocytes or isolated CD4+ T cells. A WT whole splenocyte reconstitution group was included as an additional control for comparisons with the mSOD1 whole splenocyte group. The same genes as above were examined. The statistical analysis was conducted separately for these two experiments because this study was designed to address two separate, but related, questions.

Analysis of β_{II}-*tubulin* mRNA expression in the experimental groups revealed that postoperative time had significant effects ($F_{3,54} = 112.25$, $p < 0.001$). In the RAG-2$^{-/-}$ group that received adoptive transfer of WT whole splenocytes, expression of β_{II}-*tubulin* was significantly increased relative to unoperated controls at 7, 14, and 28 dpo (160 ± 12%, 216 ± 9%, and 127 ± 20%, respectively; $p < 0.05$), and levels returned to baseline at 56 dpo. In the RAG-2$^{-/-}$ group that received adoptive transfer of mSOD1 whole splenocytes, β_{II}-*tubulin* expression was significantly elevated relative to unoperated controls at 7, 14, and 28 dpo (193 ± 34%, 206 ± 21%, and 113 ± 31%, respectively; $p < 0.05$), and expression was not different compared to control at 56 dpo. In the RAG-2$^{-/-}$ group with adoptive transfer of

mSOD1 CD4+ T cells, *β_{II}-tubulin* expression was significantly higher relative to unoperated controls at 7, 14, and 28 dpo (162 ± 7%, 200 ± 19%, and 134 ± 9%, respectively; $p < 0.05$), and expression reverted to uninjured levels at 56 dpo. In comparing whole splenocyte recipient groups, there were no statistically significant differences in the *β_{II}-tubulin* gene expression response between RAG-2$^{-/-}$ mice reconstituted with WT or mSOD1 whole splenocytes. In addition, there were no differences in *β_{II}-tubulin* expression between mSOD1 whole splenocyte or mSOD1 CD4+ T cell recipients. In comparing RAG-2$^{-/-}$ + WT whole splenocyte and RAG-2$^{-/-}$ + mSOD1 CD4+ T cell groups, there was a significant difference in *β_{II}-tubulin* expression at 7 dpo ($p = 0.036$, Fig. 5A).

Comparison of *Gap-43* mRNA expression in the experimental groups revealed that both group and postoperative time had significant effects ($F_{2,55} = 4.62$, $p = 0.014$; $F_{3,55} = 32.06$, $p < 0.001$). In the RAG-2$^{-/-}$ group that received adoptive transfer of WT whole splenocytes, expression of *Gap-43* was significantly increased relative to unoperated controls at 7, 14, and 28 dpo (1552 ± 129%, 2064 ± 258%, and 1075 ± 305%, respectively; $p < 0.05$), and levels returned to baseline at 56 dpo. In the RAG-2$^{-/-}$ group that received adoptive transfer of mSOD1 whole splenocytes, *Gap-43* expression was significantly elevated relative to unoperated controls at 7, 14, and 28 dpo (3412 ± 662%, 2845 ± 470%, and 1370 ± 373%, respectively; $p < 0.05$), and expression was not different compared to baseline at 56 dpo. In the RAG-2$^{-/-}$ group with adoptive transfer of mSOD1 CD4+ T cells, *Gap-43* expression was significantly higher relative to unoperated controls at 7 and 14 dpo (2122 ± 293% and 3064 ± 395%, respectively; $p < 0.05$), and expression reverted to uninjured levels at 28 and 56 dpo. In comparing whole splenocyte recipient groups, there was a statistically significant difference in the *Gap-43* gene expression response between RAG-2$^{-/-}$ mice reconstituted with WT or mSOD1 whole splenocytes at 7 dpo ($p = 0.002$). In addition, there was a significant difference in *Gap-43* expression between mSOD1 whole splenocyte and mSOD1 CD4+ T cell recipients at 7 dpo ($p = 0.019$). In comparing RAG-2$^{-/-}$ + WT whole splenocyte and RAG-2$^{-/-}$ + mSOD1 CD4+ T cell groups, there was a significant difference in *Gap-43* expression at 14 dpo ($p = 0.008$, Fig. 5B).

Overall, there were no significant differences in motoneuron regeneration-associated gene expression between mSOD1 and WT whole splenocyte recipients, except for increased *Gap-43* expression in the early post-axotomy timepoints. In addition, the mSOD1 whole splenocyte and mSOD1 CD4+ T cell recipients exhibited similar neuroregenerative responses, indicating that mSOD1 whole splenocytes do not have a deleterious effect on the axotomized FMN.

3.6. Axotomy-induced glial gene expression in immunodeficient mice with mSOD1 immunoreconstitution

Analysis of *Gfap* mRNA expression in the experimental groups revealed that postoperative time had significant effects ($F_{3,54} = 5.76$, $p = 0.002$). All three groups exhibited a significant increase in *Gfap* expression relative to uninjured controls at 7, 14, 28, and 56 dpo (RAG-2$^{-/-}$ + WT whole splenocytes: 2234 ± 213%, 2313 ± 255%, 2175 ± 435%, and 1492 ± 4%; RAG-2$^{-/-}$ + mSOD1 whole splenocytes: 2205 ± 178%, 2681 ± 572%, 2080 ± 446%, and 1116 ± 254%; RAG-2$^{-/-}$ + mSOD1 CD4+ T cells: 2203 ± 385%, 3138 ± 270%, 2969

± 313%, and 1859 ± 515%, respectively; $p < 0.05$). Comparing all three experimental groups reveals no significant differences in *Gfap* expression after axotomy (Fig. 6A).

Examination of *Cd68* mRNA expression in the experimental groups revealed that postoperative time had significant effects ($F_{3,54} = 11.68$, $p < 0.001$). For all three groups, *Cd68* expression was significantly increased relative to unoperated controls at 7, 14, 28, and 56 dpo (RAG-2$^{-/-}$ + WT whole splenocytes: 811 ± 55%, 606 ± 49%, 636 ± 92%, and 402 ± 106%; RAG-2$^{-/-}$ + mSOD1 whole splenocytes: 857 ± 155%, 925 ± 125%, 920 ± 207%, and 361 ± 76%; RAG-2$^{-/-}$ + mSOD1 CD4+ T cells: 772 ± 127%, 725 ± 37%, 1063 ± 99%, and 335 ± 63%, respectively; $p < 0.05$; Fig. 6B). There was a significant difference in *Cd68* expression at 28 dpo between the RAG-2$^{-/-}$ + mSOD1 CD4+ T cell and WT whole splenocyte recipients ($p = 0.002$). There were no other significant differences of *Cd68* responses between the groups at any of the observed timepoints (Fig. 6B).

To summarize, the astrocyte and microglia reaction to FNA were similar between the WT and mSOD1 whole splenocyte recipients, as well as between the mSOD1 whole splenocyte and mSOD1 CD4+ T cells recipients, indicating that mSOD1 whole splenocytes do not negatively impact the glial response to axotomy. There is a notable increase in astrocyte activation in these three group relative to the WT group (Fig. 2A).

3.7. Axotomy-induced TNF axis gene expression in immunodeficient mice with mSOD1 immunoreconstitution

Analysis of *Tnfα* mRNA expression in the experimental groups revealed that postoperative time had significant effects ($F_{3,61} = 10.63$, $p < 0.001$), and there was a significant interaction between group × postoperative time ($F_{9,61} = 2.53$, $p = 0.016$). In the RAG-2$^{-/-}$ group that received adoptive transfer of WT whole splenocytes, expression of *Tnfα* was significantly increased relative to unoperated controls at 7 and 28 dpo (2.7 ± 0.7 and 3.5 ± 1.2, respectively; $p < 0.05$), and levels were not different from baseline at 14 and 56 dpo. Both RAG-2$^{-/-}$ + mSOD1 whole splenocytes and mSOD1 CD4+ T cells groups have significantly increased *Tnfα* expression compared to unoperated controls at 7, 14, and 28 dpo (RAG-2$^{-/-}$ + mSOD1 whole splenocytes: 2.2 ± 0.6, 2.7 ± 1.3, and 3.7 ± 0.4; RAG-2$^{-/-}$ + mSOD1 CD4+ T cells: 2.3 ± 0.2, 2.3 ± 0.3, 3.1 ± 0.8, respectively; $p < 0.05$). Comparing all three experimental groups reveals no significant differences in *Tnfα* expression after axotomy (Fig. 7A).

Comparison of *Tnfr1* mRNA expression in the experimental groups revealed that postoperative time had significant effects ($F_{3,54} = 17.35$, $p < 0.001$). For all three groups, *Tnfr1* expression was significantly increased relative to unoperated controls at 7, 14, 28, and 56 dpo (RAG-2$^{-/-}$ + WT whole splenocytes: 84 ± 2%, 96 ± 4%, 86 ± 17%, and 34 ± 8%; RAG-2$^{-/-}$ + mSOD1 whole splenocytes: 108 ± 5%, 102 ± 13%, 95 ± 13%, and 44 ± 9%; RAG-2$^{-/-}$ + mSOD1 CD4+ T cells: 88 ± 7%, 102 ± 11%, 91 ± 16%, and 52 ± 9%, respectively; $p < 0.05$). There were no significant differences in *Tnfr1* expression between the three groups at any of the observed timepoints (Fig. 7B).

The data demonstrate that *Tnfα/Tnfr1* expression after FNA was equivalent between the WT and mSOD1 whole splenocyte recipients, as well as between the mSOD1 whole splenocyte

and mSOD1 CD4+ T cells recipients, indicating that mSOD1 whole splenocytes do not affect the axotomy-induced TNF axis response.

3.8. Axotomy-induced Fas/nNos cell death signaling pathway gene expression in immunodeficient mice with mSOD1 immunoreconstitution

Analysis of *Fas* mRNA expression in the experimental groups revealed that group and postoperative time had significant effects ($F_{2,54} = 6.01$, $p = 0.004$; $F_{3,54} = 14.92$, $p < 0.001$), and there was a significant interaction between group × postoperative time ($F_{6,54} = 2.58$, $p = 0.029$). In the RAG-2$^{-/-}$ group that received adoptive transfer of WT whole splenocytes, expression of *Fas* was not significantly different from unoperated controls at any of the examined timepoints. In the RAG-2$^{-/-}$ group that received adoptive transfer of mSOD1 whole splenocytes, *Fas* expression was significantly elevated relative to unoperated controls at 7, 14, 28, and 56 dpo (72 ± 23%, 55 ± 9%, 133 ± 23%, and 82 ± 9%, respectively; $p < 0.05$). In the RAG-2$^{-/-}$ group with adoptive transfer of mSOD1 CD4+ T cells, *Fas* expression remained at baseline levels at 7 and 14 dpo, then increased significantly relative to unoperated controls at 28 and 56 dpo (191 ± 32% and 81 ± 15%, respectively; $p < 0.05$). In comparing the WT and mSOD1 whole splenocyte recipient groups, there were statistically significant differences in *Fas* gene expression at 7 and 28 dpo ($p = 0.025$ and 0.013, respectively). Additionally, there was a significant difference between RAG-2$^{-/-}$ + WT whole splenocyte and mSOD1 CD4+ T cell recipients at 28 dpo ($p < 0.001$). There was also a significant increase in *Fas* expression at 28 dpo between mSOD1 CD4+ T cell recipients compared to mSOD1 whole splenocyte recipients ($p = 0.038$; Fig. 8A).

Comparison of *nNos* mRNA expression in the experimental groups revealed that postoperative time had significant effects ($F_{3,54} = 3.83$, $p = 0.015$). In the RAG-2$^{-/-}$ group that received adoptive transfer of WT whole splenocytes or mSOD1 CD4+ T cells, expression levels of *nNos* were not significantly different from unoperated controls at any of the examined timepoints. In the RAG-2$^{-/-}$ group that received adoptive transfer of mSOD1 whole splenocytes, *nNos* expression was significantly elevated relative to unoperated controls at 56 dpo (62 ± 20, $p < 0.05$). In comparing WT and mSOD1 whole splenocyte recipient groups, there were no statistically significant differences in the *nNos* gene expression response. There was a significant difference in *nNos* expression at 14 dpo between RAG-2$^{-/-}$ + WT whole splenocyte and RAG-2$^{-/-}$+ mSOD1 CD4+ T cell groups ($p = 0.031$). Comparing RAG-2$^{-/-}$ groups that received adoptive cell transfer of mSOD1 whole splenocytes or mSOD1 CD4+ T cells reveals significant differences in *nNos* expression at 7 and 56 dpo ($p = 0.030$ and 0.020, respectively; Fig. 8B).

After FNA, both mSOD1 whole splenocytes and mSOD1 CD4+ T cell recipients have elevated central Fas expression at 28 dpo, and mSOD1 whole splenocytes also increased Fas at 7 dpo compared to WT whole splenocytes. nNos expression was also increased in mSOD1 whole splenocyte recipients at 7 and 56 dpo relative to mSOD1 CD4+ T cell recipients. Together, these findings indicate that the mSOD1 gene mutation restricted to the peripheral immune system compartment results in aberrant induction of Fas/nNos expression after FNA, potentially leading to increased FMN death after target disconnection.

4. Discussion

4.1. Summary of findings

Historically, the CNS response to peripheral target disconnection has been well-characterized and collectively described as the “axon reaction” and/or “nerve cell body response to injury” (Lieberman, 1971; Grafstein, 1975). Using a variety of techniques, including *in situ* hybridization, PCR, protein quantitation, and immunohistochemistry, coordinated neuronal/glial RNA and protein changes have been documented in the facial nerve injury model in particular and were verified here in additional control experiments that are presented in the supplementary data section (Figs. S1 and 2). In the present study, we capitalized on this wealth of foundational literature in the design and utilization of laser capture microdissection and qPCR to examine the impact of immunodeficiency on gene expression in the facial motor nucleus after peripheral target disconnection. While the phenotypic MN response to nerve injury was not altered, astrocytic and microglial responses were specifically affected by peripheral immune status. Importantly, elevated Fas gene expression within the facial nucleus after axotomy occurred with reconstitution using immune cells from the mSOD1 mice, suggesting a unique immune defect capable of inducting motoneuron-specific central death mechanisms.

4.2. Intrinsic motoneuron molecular response to injury is not affected by peripheral immunestatus

4.2.1. CD4+ T cell-mediated neuroprotection does not occur via regulation of motoneuron regeneration-associated gene expression—To determine if CD4+ T cells acted directly on the motoneuron to promote neuronal survival after axotomy, we examined the effects of peripheral immune status on the motoneuron cell body response to axotomy. Neither immunodeficiency nor reconstitution with WT CD4+ T cells resulted in significant changes in the motoneuron gene expression response to axotomy, indicating that the motoneuron molecular response occurs independent from the peripheral immune system. Further evidence that motoneuron regeneration after axotomy is unaffected by peripheral immune status can be found in studies using crush axotomy, in which slowed, but complete, functional recovery is observed in immunodeficient or immunosuppressed mice (Lieberman et al., 2011; Bombeiro et al., 2016). In both crush and cut axotomies, significantly more motoneuron death is observed in immunodeficient and immunosuppressed mice, despite the regenerative efforts of the motoneuron (Serpe et al., 1999; Beahrs et al., 2010; Lieberman et al., 2011). This incongruency between the motoneuron regeneration response and cell body survival supports the concept that factors extrinsic to the motoneuron are responsible for determining motoneuron survival after injury.

4.2.2. mSOD1 whole splenocytes do not negatively affect motoneuron regeneration-associated gene expression—The failure of mSOD1 whole splenocytes to confer neuroprotection in immunodeficient mice, despite their containing neuroprotective mSOD1 CD4+ T cells, led us examine how neuroregenerative molecular responses to axotomy were affected by mSOD1 whole splenocytes. Overall, mSOD1 whole splenocyte recipients exhibited a similar motoneuron regeneration-associated gene expression response relative to WT whole splenocyte and mSOD1 CD4+ T cell recipients,

indicating that mSOD1 whole splenocytes do not have a negative effect on the motoneuron response to axotomy. This finding corroborates molecular data gathered from axotomized mSOD1 mice, which also demonstrate WT-levels of regeneration-associated gene expression after axotomy but significantly greater motoneuron death (Mariotti et al., 2002; Mesnard et al., 2011; Kawamura et al., 2012; Haulcomb et al., 2014). Similar to immunodeficient mice, mSOD1 mice have delayed, but complete, functional recovery after a crush axotomy, suggesting that the intrinsic neuroregeneration response to axotomy is also intact in the context of motoneuron disease (Mesnard et al., 2013).

These results collectively indicate that the axotomy-induced motoneuron regeneration response is an intrinsic program executed by the motoneuron that is not affected by motoneuron disease or peripheral immune status. Additionally, this disconnect between increased motoneuron death and intact neuroregenerative responses supports the claim that extrinsic, not intrinsic, components dictate motoneuron survival after injury.

4.3. Extrinsic glial molecular response to injury is significantly affected by peripheral immune status

4.3.1. WT CD4+ T cells are responsible for sustaining the glial activation response to axotomy—In examining the effects of immune status on astrocyte and microglia gene expression after axotomy, it was discovered that in immunodeficient mice, glial activation is initially intact, however prematurely falls to baseline levels relative to WT. The astrocyte reaction is more sensitive to immune status because their decreased activation is observed at both middle and late post-axotomy timepoints, whereas decreased microglia activation is observed only at a later timepoint. Adoptive transfer of WT CD4+ T cells fully restores astrocyte and microglia activation to WT levels, signifying that the peripheral immune system regulates central glial activation after axotomy.

Our findings of intact early glial responses to injury are in agreement with the literature describing that initiation of the glial reaction occurs in response to electrical signals, purine release, and cytokine signaling from the injured motoneuron cell body (Grafstein, 1975; Streit et al., 2000; Castellano et al., 2016). The timing of the loss of glial activation at middle and late timepoints correlates with peak production of T_H2-inducing cytokines and maximum T cell presence found by other studies of the post-axotomy facial motor nucleus (Raivich et al., 1998; Wainwright et al., 2009a; Almolda et al., 2014). This glial activation by CD4+ T cells may occur in response to the secondary reactivation of CD4+ T cells by APCs in the CNS (Aloisi et al., 1999; Carson et al., 1999; Byram et al., 2004).

The sensitivity of astrocyte activation to the lack of CD4+ T cells is evident in other neurodegenerative disease models. For example, decreased astrogliosis and unaffected microgliosis is observed in a RAG-$2^{-/-}$/PSAPP (presenilin 1/amyloid precursor protein) transgenic mouse model of Alzheimer's disease (Spani et al., 2015). A similar pattern of decreased astrocyte and intact microglia activation is observed in $CD4^{-/-}$ mice after spinal nerve L5 transection (Cao & DeLeo, 2008). Microglia in severe combined immunodeficient (scid) mice form more phagocytic clusters and have decreased expression of MHC I antigen-presenting molecules in response to FNA, demonstrating that some microglia responses are reliant upon the adaptive arm of the immune system (Bohatschek et al., 2004a). Altogether,

our results, combined with findings in the literature, lead us to conclude that the central glial reaction to peripheral nerve injury is reliant upon CD4+ T cells.

4.3.2. mSOD1 whole splenocytes do not inhibit mSOD1 CD4+ T cell regulation of the glial activation response, but may differentially induce a neurotoxic glial phenotype—

Previous studies identified that mSOD1 mice exhibit decreased glial reaction relative to WT mice after FNA, similar to what is observed in immunodeficient RAG-2$^{-/-}$ mice in the first half of this study (Mesnard et al., 2011; Haulcomb et al., 2014). These results led us to hypothesize that mSOD1 whole splenocytes would inhibit the ability of mSOD1 CD4+ T cells to regulate the glial response to injury. To our surprise, glial activation in mSOD1 whole splenocyte recipients were similar to WT whole splenocyte and mSOD1 CD4+ T cell recipients, leading us to reject our original hypothesis. In fact, a significant augmentation of the axotomy-induced astrocyte response was observed in these three experimental groups relative to WT and WT CD4+ T cell recipient groups, supporting the concept that astrocytes are acutely sensitive to peripheral immune status.

Future experiments will further characterize the phenotypic responses of astrocytes and microglia to FNA because *Gfap* and *Cd68* gene expression are pan-activation markers of glial responses (Laskawi & Wolff, 1996; Brettschneider et al., 2012). Examination of the astrocyte phenotypic response is of particular importance to future work given the significant effects peripheral immune status has on astrocyte reaction to FNA. Recent transcriptomic analyses of astrocytes in different neurological disease contexts identified neurotoxic A1 and neuroprotective A2 astrocyte phenotypes (Zamanian et al., 2012; Liddelow et al., 2017). These studies, in conjunction with our data, lead us to hypothesize that mSOD1 whole splenocytes may promote the neurotoxic A1 phenotype, whereas mSOD1 CD4+ T cells promote the neuroprotective A2 phenotype, and this differential regulation of astrocytic phenotype may be a key determinant of motoneuron survival after axotomy.

4.4. A novel role for TNFα signaling in the post-axotomy facial motor nucleus

4.4.1. WT CD4+ T cells may regulate glial microenvironment responses using the TNFa signaling pathway—

Because immunodeficient mice have greater motoneuron death after axotomy, expression of *Tnfα/Tnfr1* was analyzed in this study because previous studies identified that TNFα is associated with FMN death after FNA (Terrado et al., 2000; Raivich, 2002). In this study, immunodeficient mice demonstrated a decreased *Tnfα* and delayed *Tnfr1* response, suggesting that TNFα signaling is not contributing to the increased motoneuron death observed in this group. Furthermore, WT CD4+ T cells both restored and augmented *Tnfα* expression, and also elicited a significant increase in *Tnfr1* expression relative to both WT and immunodeficient mice, leading us to conclude that CD4+ T cells may regulate glial microenvironment responses via the TNFα/TNFR1 signaling pathway. This signaling pathway is important for regulation of cytokine production and inflammatory responses (Baud & Karin, 2001; McCoy & Tansey, 2008; Wajant & Scheurich, 2011). In the CNS, TNFα promotes astrocyte connectivity, and it also regulates nitric oxide production and antigen presentation by microglia (Hensley, 2003; Almad et al., 2016) (Bohatschek et al., 2004a). Altogether, we conclude that WT CD4+ T cells potentially utilize the TNF

signaling axis to regulate glial responses to peripheral nerve axotomy to promote motoneuron survival.

4.4.2. mSOD1 whole splenocytes do not induce TNF-mediated cell death in the post-axotomy facial motor nucleus—TNFα can have both beneficial and harmful roles in the CNS, and in the context of the mSOD1 mouse model, neuroinflammation is observed early in disease pathology and is associated with greater motoneuron death (Alexianu et al., 2001; Hensley et al., 2002; Hensley, 2003; Chen et al., 2004). In the control facial motor nucleus of mSOD1 mice, constitutive expression of *Tnfa* is observed as early as postnatal day 59, and FMN death from disease alone is observed as early as postnatal day 112 (Mesnard et al., 2011; Haulcomb et al., 2014). In this study, we examined if mSOD1 whole splenocytes promoted FMN death after FNA by induction of the TNFα/TNFR1 death pathway. First, neither mSOD1 whole splenocytes nor mSOD1 CD4+ T cells induced *Tnfa* expression in the control facial motor nucleus, suggesting that the constitutive TNFα observed in mSOD1 mice is not induced by the peripheral immune system. After axotomy, there were no differences in *Tnfa/Tnfr1* expression when comparing mSOD1 whole splenocyte, WT whole splenocyte, and mSOD1 CD4+ T cell recipient groups, indicating that mSOD1 whole splenocytes do not utilize this signaling pathway to promote motoneuron death. To summarize, the TNF signaling axis is not associated with motoneuron death induced by mSOD1 whole splenocytes.

4.5. mSOD1 disease mutation restricted to the peripheral immune compartment induces central Fas/nNos expression

4.5.1. Fas/nNos-mediated motoneuron death is not associated with axotomy-induced motoneuron death in immunodeficient mice—Fas and Fas ligand (FasL) are ubiquitously expressed in the CNS and are utilized to prevent autoimmune reactions in the brain (Flugel et al., 2000; Becher et al., 2006). Fas and FasL can also induce neuronal death in the context of many different neurological diseases, and it is highly associated with pathological motoneuron death in the mSOD1 mouse model of ALS (Raoul et al., 2002; Choi & Benveniste, 2004; Raoul et al., 2006; Locatelli et al., 2007). Downstream signaling from Fas can activate nNos, a neuron-specific terminal step of Fas-mediated cell death in the CNS (Raoul et al., 2002).

When the Fas/nNos death pathway was examined in immunodeficient mice, there were no significant increases in expression of either of these death pathway components. WT CD4+ T cells also did not significantly alter expression of these molecules in the post-axotomy timecourse. Altogether, these results indicate that the increased axotomy-induced motoneuron death in immunodeficient mice is not due to the Fas cell death pathway, and is likely the result of dysregulation of extrinsic factors that promote motoneuron survival.

4.5.2. mSOD1 whole splenocytes and mSOD1 CD4+ T cells significantly increase expression of Fas—mSOD1 mice have a significant upregulation of the Fas/nNos death pathway after axotomy, providing further evidence that Fas-induced cell death may be an important contributor to disease pathology (Haulcomb et al., 2014). In examining Fas expression in this study, both mSOD1 whole splenocyte and mSOD1 CD4+ T cell

recipient groups has increased *Fas* expression relative to WT whole splenocyte recipient controls. *nNos* expression was also increased in the mSOD1 whole splenocyte group, and this increase was significant relative to the mSOD1 CD4+ T cell recipients at both early and late post-axotomy timepoints. These findings lead us to conclude that the presence of the mSOD1 mutation in the peripheral immune system compartment alone can result in induction of central neuronal death mechanisms after peripheral nerve injury.

To confirm these results, future experiments will determine if disrupting the Fas-mediated death pathway blocks mSOD1 whole splenocyte-induced motoneuron death, using a similar approach as performed on mSOD1 mice (Raoul et al., 2006). Additionally, the cell-specific downstream effects of Fas-signaling will need to be examined in both mSOD1 CD4+ T cell and mSOD1 whole splenocyte recipients to determine the differential effects these immunoreconstitutions have that contribute to motoneuron survival or death.

4.6 Potential clinical applications of findings

In this study, we demonstrate that the peripheral immune system significantly regulates central molecular responses to peripheral nerve injury, which carries implications for future clinical therapies for ALS. Clinical trials targeting the immune system in ALS have largely focused on immunosuppression, which, as shown here, can result in loss of both the neuroprotective and neurotoxic effects (Kelemen et al., 1983; Brown et al., 1986; Werdelin et al., 1990; Drachman et al., 1994). With the mounting evidence supporting the non-cell autonomous theory of ALS, the results of this study lead us to hypothesize that the peripheral immune system may be a key contributor to motoneuron death in ALS, through both the induction of a neurotoxic A1 astrocyte phenotype and promotion of Fas cell death receptor expression in the CNS (Fig. 9). The results of this study, in combination with our previously published series of papers (Mesnard et al., 2010; Mesnard et al., 2011; Haulcomb et al., 2014), have led to the successful identification of key CNS cellular and molecular targets regulated by peripheral immune status in response to peripheral nerve injury. Future directions will include dissection of the combination of cell-cell interactions and regulatory pathways using genetic manipulation and protein analysis to identify clinically-relevant therapeutic targets.

Supplementary Material

Refer to Web version on PubMed Central for supplementary material.

Acknowledgments

This work was supported by a research grant from the National Institute of Health (NS40433; KJJ and VMS)

References

Alexianu ME, Kozovska M, Appel SH. Immune reactivity in a mouse model of familial ALS correlates with disease progression. Neurology. 2001; 57(7):1282–1289. [PubMed: 11591849]

Almad AA, Doreswamy A, Gross SK, Richard JP, Huo Y, Haughey N, Maragakis NJ. Connexin 43 in astrocytes contributes to motor neuron toxicity in amyotrophic lateral sclerosis. Glia. 2016; 64(7): 1154–1169. DOI: 10.1002/glia.22989 [PubMed: 27083773]

Almolda B, Villacampa N, Manders P, Hidalgo J, Campbell IL, Gonzalez B, Castellano B. Effects of astrocyte-targeted production of interleukin-6 in the mouse on the host response to nerve injury. Glia. 2014; 62(7):1142–1161. DOI: 10.1002/glia.22668 [PubMed: 24691898]

Aloisi F, Ria F, Columba-Cabezas S, Hess H, Penna G, Adorini L. Relative efficiency of microglia, astrocytes, dendritic cells and B cells in naive CD4+ T cell priming and Th1/Th2 cell restimulation. Eur J Immunol. 1999; 29(9):2705–2714. DOI: 10.1002/(SICI)1521-4141(199909)29:09<2705::AID-IMMU2705>3.0.CO;2-1 [PubMed: 10508245]

Alvarez ML, Done SC. SYBR(R) Green and TaqMan(R) quantitative PCR arrays: expression profile of genes relevant to a pathway or a disease state. Methods Mol Biol. 2014; 1182:321–359. DOI: 10.1007/978-1-4939-1062-5_27 [PubMed: 25055922]

Armstrong BD, Abad C, Chhith S, Cheung-Lau G, Hajji OE, Nobuta H, Waschek JA. Impaired nerve regeneration and enhanced neuroinflammatory response in mice lacking pituitary adenylyl cyclase activating peptide. Neuroscience. 2008; 151(1):63–73. DOI: 10.1016/j.neuroscience.2007.09.084 [PubMed: 18055122]

Banerjee R, Mosley RL, Reynolds AD, Dhar A, Jackson-Lewis V, Gordon PH, et al. Gendelman HE. Adaptive immune neuroprotection in G93A-SOD1 amyotrophic lateral sclerosis mice. PLoS One. 2008; 3(7):e2740.doi: 10.1371/journal.pone.0002740 [PubMed: 18648532]

Baud V, Karin M. Signal transduction by tumor necrosis factor and its relatives. Trends Cell Biol. 2001; 11(9):372–377. [PubMed: 11514191]

Beahrs T, Tanzer L, Sanders VM, Jones KJ. Functional recovery and facial motoneuron survival are influenced by immunodeficiency in crush-axotomized mice. Exp Neurol. 2010; 221(1):225–230. DOI: 10.1016/j.expneurol.2009.11.003 [PubMed: 19913014]

Becher B, Bechmann I, Greter M. Antigen presentation in autoimmunity and CNS inflammation: how T lymphocytes recognize the brain. J Mol Med (Berl). 2006; 84(7):532–543. DOI: 10.1007/s00109-006-0065-1 [PubMed: 16773356]

Beers DR, Henkel JS, Zhao W, Wang J, Appel SH. CD4+ T cells support glial neuroprotection, slow disease progression, and modify glial morphology in an animal model of inherited ALS. Proc Natl Acad Sci U S A. 2008; 105(40):15558–15563. DOI: 10.1073/pnas.0807419105 [PubMed: 18809917]

Bohatschek M, Kloss CU, Hristova M, Pfeffer K, Raivich G. Microglial major histocompatibility complex glycoprotein-1 in the axotomized facial motor nucleus: regulation and role of tumor necrosis factor receptors 1 and 2. J Comp Neurol. 2004a; 470(4):382–399. DOI: 10.1002/cne.20017 [PubMed: 14961564]

Bohatschek M, Kloss CU, Pfeffer K, Bluethmann H, Raivich G. B7.2 on activated and phagocytic microglia in the facial axotomy model: regulation by interleukin-1 receptor type 1, tumor necrosis factor receptors 1 and 2 and endotoxin. J Neuroimmunol. 2004b; 156(1-2):132–145. DOI: 10.1016/j.jneuroim.2004.07.018 [PubMed: 15465604]

Bombeiro AL, Santini JC, Thome R, Ferreira ER, Nunes SL, Moreira BM, et al. Oliveira AL. Enhanced Immune Response in Immunodeficient Mice Improves Peripheral Nerve Regeneration Following Axotomy. Front Cell Neurosci. 2016; 10:151.doi: 10.3389/fncel.2016.00151 [PubMed: 27378849]

Brettschneider J, Toledo JB, Van Deerlin VM, Elman L, McCluskey L, Lee VM, Trojanowski JQ. Microglial activation correlates with disease progression and upper motor neuron clinical symptoms in amyotrophic lateral sclerosis. PLoS One. 2012; 7(6):e39216.doi: 10.1371/journal.pone.0039216 [PubMed: 22720079]

Brown RH Jr, Hauser SL, Harrington H, Weiner HL. Failure of immunosuppression with a ten- to 14-day course of high-dose intravenous cyclophosphamide to alter the progression of amyotrophic lateral sclerosis. Arch Neurol. 1986; 43(4):383–384. [PubMed: 3954622]

Byram SC, Carson MJ, DeBoy CA, Serpe CJ, Sanders VM, Jones KJ. CD4-positive T cell-mediated neuroprotection requires dual compartment antigen presentation. J Neurosci. 2004; 24(18):4333–4339. DOI: 10.1523/jneurosci.5276-03.2004 [PubMed: 15128847]

Cao L, DeLeo JA. CNS-infiltrating CD4+ T lymphocytes contribute to murine spinal nerve transection-induced neuropathic pain. Eur J Immunol. 2008; 38(2):448–458. DOI: 10.1002/eji.200737485 [PubMed: 18196515]

Carson MJ, Sutcliffe JG, Campbell IL. Microglia stimulate naive T-cell differentiation without stimulating T-cell proliferation. J Neurosci Res. 1999; 55(1):127–134. DOI: 10.1002/(SICI)1097-4547(19990101)55:1<127::AID-JNR14>3.0.CO;2-2 [PubMed: 9890441]

Castellano B, Bosch-Queralt M, Almolda B, Villacampa N, Gonzalez B. Purine Signaling and Microglial Wrapping. Adv Exp Med Biol. 2016; 949:147–165. DOI: 10.1007/978-3-319-40764-7_7 [PubMed: 27714688]

Chen LC, Smith A, Ben Y, Zukic B, Ignacio S, Moore D, Lee N. Temporal gene expression patterns in G93A/SOD1 mouse. Amyotroph Lateral Scler Other Motor Neuron Disord. 2004; 5(3):164–171. DOI: 10.1080/14660820410017091 [PubMed: 15512905]

Chen X, Feng W, Huang R, Guo X, Chen Y, Zheng Z, Shang H. Evidence for peripheral immune activation in amyotrophic lateral sclerosis. J Neurol Sci. 2014; 347(1-2):90–95. DOI: 10.1016/j.jns.2014.09.025 [PubMed: 25312013]

Choi C, Benveniste EN. Fas ligand/Fas system in the brain: regulator of immune and apoptotic responses. Brain Research Reviews. 2004; 44(1):65–81. DOI: 10.1016/j.brainresrev.2003.08.007 [PubMed: 14739003]

DeFrancesco-Lisowitz A, Lindborg JA, Niemi JP, Zigmond RE. The neuroimmunology of degeneration and regeneration in the peripheral nervous system. Neuroscience. 2015; 302:174–203. DOI: 10.1016/j.neuroscience.2014.09.027 [PubMed: 25242643]

Drachman DB, Chaudhry V, Cornblath D, Kuncl RW, Pestronk A, Clawson L, et al. Trial of immunosuppression in amyotrophic lateral sclerosis using total lymphoid irradiation. Ann Neurol. 1994; 35(2):142–150. DOI: 10.1002/ana.410350205 [PubMed: 8109895]

Edwards DA. Mice: fighting by neonatally androgenized females. Science. 1968; 161(3845):1027–1028. [PubMed: 5691460]

Flugel A, Schwaiger FW, Neumann H, Medana I, Willem M, Wekerle H, et al. Graeber MB. Neuronal FasL induces cell death of encephalitogenic T lymphocytes. Brain Pathol. 2000; 10(3):353–364. [PubMed: 10885654]

Graeber MB, Tetzlaff W, Streit WJ, Kreutzberg GW. Microglial cells but not astrocytes undergo mitosis following rat facial nerve axotomy. Neurosci Lett. 1988; 85(3):317–321. [PubMed: 3362421]

Grafstein B. The nerve cell body response to axotomy. Exp Neurol. 1975; 48(3pt. 2):32–51. [PubMed: 1102323]

Haulcomb MM, Mesnard NA, Batka RJ, Alexander TD, Sanders VM, Jones KJ. Axotomy-induced target disconnection promotes an additional death mechanism involved in motoneuron degeneration in amyotrophic lateral sclerosis transgenic mice. J Comp Neurol. 2014; 522(10):2349–2376. DOI: 10.1002/cne.23538 [PubMed: 24424947]

Hensley K. Message and protein-level elevation of tumor necrosis factor α (TNFα) and TNFα-modulating cytokines in spinal cords of the G93A-SOD1 mouse model for amyotrophic lateral sclerosis. Neurobiology of Disease. 2003; 14(1)(03):74–80. 00087–1. DOI: 10.1016/s0969-9961 [PubMed: 13678668]

Hensley K, Floyd RA, Gordon B, Mou S, Pye QN, Stewart C, et al. Williamson K. Temporal patterns of cytokine and apoptosis-related gene expression in spinal cords of the G93A-SOD1 mouse model of amyotrophic lateral sclerosis. J Neurochem. 2002; 82(2):365–374. [PubMed: 12124437]

Ip CW, Beck SK, Volkmann J. Lymphocytes reduce nigrostriatal deficits in the 6-hydroxydopamine mouse model of Parkinson's disease. J Neural Transm (Vienna). 2015; 122(12):1633–1643. DOI: 10.1007/s00702-015-1444-y [PubMed: 26290125]

Kamakura R, Kovalainen M, Leppaluoto J, Herzig KH, Makela KA. The effects of group and single housing and automated animal monitoring on urinary corticosterone levels in male C57BL/6 mice. Physiol Rep. 2016; 4(3)doi: 10.14814/phy2.12703

Kawamura MF, Yamasaki R, Kawamura N, Tateishi T, Nagara Y, Matsushita T, et al. Kira J. Impaired recruitment of neuroprotective microglia and T cells during acute neuronal injury coincides with increased neuronal vulnerability in an amyotrophic lateral sclerosis model. Exp Neurol. 2012; 234(2):437–445. DOI: 10.1016/j.expneurol.2012.01.015 [PubMed: 22293437]

Kelemen J, Hedlund W, Orlin JB, Berkman EM, Munsat TL. Plasmapheresis with immunosuppression in amyotrophic lateral sclerosis. Arch Neurol. 1983; 40(12):752–753. [PubMed: 6625990]

Kuzmenok OI, Sanberg PR, Desjarlais TG, Bennett SP, Garbuzova-Davis SN. Lymphopenia and spontaneous autorosette formation in SOD1 mouse model of *ALS*. J Neuroimmunol. 2006; 172(1-2):132–136. DOI: 10.1016/j.jneuroim.2005.11.015 [PubMed: 16376995]

Laboratory J. Flow-cytometric analysis of 11 strains of mice. MPD:Jaxpheno6.

Laskawi R, Wolff JR. Changes in glial fibrillary acidic protein immunoreactivity in the rat facial nucleus following various types of nerve lesions. Eur Arch Otorhinolaryngol. 1996; 253(8):475–480. [PubMed: 8950547]

Liddelow SA, Guttenplan KA, Clarke LE, Bennett FC, Bohlen CJ, Schirmer L, et al. Barres BA. Neurotoxic reactive astrocytes are induced by activated microglia. Nature. 2017; 541(7638):481–487. DOI: 10.1038/nature21029 [PubMed: 28099414]

Lieberman AR. The axon reaction: a review of the principal features of perikaryal responses to axon injury. Int Rev Neurobiol. 1971; 14:49–124. [PubMed: 4948651]

Lieberman DM, Jan TA, Ahmad SO, Most SP. Effects of corticosteroids on functional recovery and neuron survival after facial nerve injury in mice. Arch Facial Plast Surg. 2011; 13(2):117–124. DOI: 10.1001/archfacial.2010.98 [PubMed: 21079107]

Locatelli F, Corti S, Papadimitriou D, Fortunato F, Del Bo R, Donadoni C, et al. Comi GP. Fas small interfering RNA reduces motoneuron death in amyotrophic lateral sclerosis mice. Ann Neurol. 2007; 62(1):81–92. DOI: 10.1002/ana.21152 [PubMed: 17503505]

Lockworth CR, Kim SJ, Liu J, Palla SL, Craig SL. Effect of Enrichment Devices on Aggression in Manipulated Nude Mice. J Am Assoc Lab Anim Sci. 2015; 54(6):731–736. [PubMed: 26632782]

Lu CH, Allen K, Oei F, Leoni E, Kuhle J, Tree T, et al. Malaspina A. Systemic inflammatory response and neuromuscular involvement in amyotrophic lateral sclerosis. Neurol Neuroimmunol Neuroinflamm. 2016; 3(4):e244.doi: 10.1212/NXI.0000000000000244 [PubMed: 27308305]

Mariotti R, Cristino L, Bressan C, Boscolo S, Bentivoglio M. Altered reaction of facial motoneurons to axonal damage in the presymptomatic phase of a murine model of familial amyotrophic lateral sclerosis. Neuroscience. 2002; 115(2):331–335. [PubMed: 12421599]

McCoy MK, Tansey MG. TNF signaling inhibition in the CNS: implications for normal brain function and neurodegenerative disease. J Neuroinflammation. 2008; 5:45.doi: 10.1186/1742-2094-5-45 [PubMed: 18925972]

Mesnard-Hoaglin NA, Xin J, Haulcomb MM, Batka RJ, Sanders VM, Jones KJ. SOD1(G93A) transgenic mouse CD4(+) T cells mediate neuroprotection after facial nerve axotomy when removed from a suppressive peripheral microenvironment. Brain Behav Immun. 2014; 40:55–60. DOI: 10.1016/j.bbi.2014.05.019 [PubMed: 24911596]

Mesnard NA, Alexander TD, Sanders VM, Jones KJ. Use of laser microdissection in the investigation of facial motoneuron and neuropil molecular phenotypes after peripheral axotomy. Exp Neurol. 2010; 225(1):94–103. DOI: 10.1016/j.expneurol.2010.05.019 [PubMed: 20570589]

Mesnard NA, Haulcomb MM, Tanzer L, Sanders VM, Jones KJ. Delayed functional recovery in presymptomatic mSOD1 mice following facial nerve crush axotomy. J Neurodegener Regen. 2013; 4(1):21–25. [PubMed: 24672589]

Mesnard NA, Sanders VM, Jones KJ. Differential gene expression in the axotomized facial motor nucleus of presymptomatic SOD1 mice. J Comp Neurol. 2011; 519(17):3488–3506. DOI: 10.1002/cne.22718 [PubMed: 21800301]

Moran LB, Graeber MB. The facial nerve axotomy model. Brain Res Brain Res Rev. 2004; 44(2-3): 154–178. DOI: 10.1016/j.brainresrev.2003.11.004 [PubMed: 15003391]

Olmstead DN, Mesnard-Hoaglin NA, Batka RJ, Haulcomb MM, Miller WM, Jones KJ. Facial nerve axotomy in mice: a model to study motoneuron response to injury. J Vis Exp. 2015; (96):e52382.doi: 10.3791/52382 [PubMed: 25742324]

Olsson IAS, Westlund K. More than numbers matter: The effect of social factors on behaviour and welfare of laboratory rodents and non-human primates. Applied Animal Behaviour Science. 2007; 103(3-4):229–254. DOI: 10.1016/j.applanim.2006.05.022

Raivich G. Cytotoxic Potential of Proinflammatory Cytokines: Combined Deletion of TNF Receptors TNFR1 and TNFR2 Prevents Motoneuron Cell Death after Facial Axotomy in Adult Mouse. Experimental Neurology. 2002; 178(2):186–193. DOI: 10.1006/exnr.2002.8024 [PubMed: 12504878]

Raivich G, Jones LL, Kloss CU, Werner A, Neumann H, Kreutzberg GW. Immune surveillance in the injured nervous system: T-lymphocytes invade the axotomized mouse facial motor nucleus and aggregate around sites of neuronal degeneration. J Neurosci. 1998; 18(15):5804–5816. [PubMed: 9671668]

Raoul C, Buhler E, Sadeghi C, Jacquier A, Aebischer P, Pettmann B, et al. Haase G. Chronic activation in presymptomatic amyotrophic lateral sclerosis (ALS) mice of a feedback loop involving Fas, Daxx, and FasL. Proc Natl Acad Sci U S A. 2006; 103(15):6007–6012. DOI: 10.1073/pnas.0508774103 [PubMed: 16581901]

Raoul C, Estevez AG, Nishimune H, Cleveland DW, deLapeyriere O, Henderson CE, et al. Pettmann B. Motoneuron death triggered by a specific pathway downstream of Fas. potentiation by ALS-linked SOD1 mutations. Neuron. 2002; 35(6):1067–1083. [PubMed: 12354397]

Serpe CJ, Coers S, Sanders VM, Jones KJ. CD4+ T, but not CD8+ or B, lymphocytes mediate facial motoneuron survival after facial nerve transection. Brain, Behavior, and Immunity. 2003; 17(5): 393–402. DOI: 10.1016/s0889-1591(03)00028-x

Serpe CJ, Kohm AP, Huppenbauer CB, Sanders VM, Jones KJ. Exacerbation of facial motoneuron loss after facial nerve transection in sever e combined immunodeficient (scid) mice. J Neurosci. 1999; 19(11):RC7. [PubMed: 10341268]

Serpe CJ, Sanders VM, Jones KJ. Kinetics of facial motoneuron loss following facial nerve transection in severe combined immunodeficient mice. J Neurosci Res. 2000; 62(2):273–278. DOI: 10.1002/1097-4547(20001015)62:2<273::AID-JNR11>3.0.CO;2-C [PubMed: 11020219]

Spani C, Suter T, Derungs R, Ferretti MT, Welt T, Wirth F, et al. Kulic L. Reduced beta-amyloid pathology in an APP transgenic mouse model of Alzheimer's disease lacking functional B and T cells. Acta Neuropathol Commun. 2015; 3:71.doi: 10.1186/s40478-015-0251-x [PubMed: 26558367]

Streit WJ, Hurley SD, McGraw TS, Semple-Rowland SL. Comparative evaluation of cytokine profiles and reactive gliosis supports a critical role for interleukin-6 in neuron-glia signaling during regeneration. J Neurosci Res. 2000; 61(1):10–20. DOI: 10.1002/1097-4547(20000701)61:1<10::aid-jnr2>3.0.co;2-e [PubMed: 10861795]

Terrado J, Monnier D, Perrelet D, Vesin D, Jemelin S, Buurman WA, et al. Garcia I. Soluble TNF receptors partially protect injured motoneurons in the postnatal CNS. Eur J Neurosci. 2000; 12(9): 3443–3447. [PubMed: 10998128]

Tetzlaff W, Alexander SW, Miller FD, Bisby MA. Response of facial and rubrospinal neurons to axotomy: changes in mRNA expression for cytoskeletal proteins and GAP-43. J Neurosci. 1991; 11(8):2528–2544. [PubMed: 1831228]

Tetzlaff W, Graeber MB, Bisby MA, Kreutzberg GW. Increased glial fibrillary acidic protein synthesis in astrocytes during retrograde reaction of the rat facial nucleus. Glia. 1988; 1(1):90–95. DOI: 10.1002/glia.440010110 [PubMed: 2976741]

Van Loo PL, Van Zutphen LF, Baumans V. Male management: Coping with aggression problems in male laboratory mice. Lab Anim. 2003; 37(4):300–313. DOI: 10.1258/002367703322389870 [PubMed: 14599305]

Wainwright DA, Mesnard NA, Xin J, Sanders VM, Jones KJ. Effects of facial nerve axotomy on Th2-associated and Th1-associated chemokine mRNA expression in the facial motor nucleus of wild-type and presymptomatic SOD1 mice. J Neurodegener Regen. 2009a; 2(1):39–44. [PubMed: 20436785]

Wainwright DA, Xin J, Mesnard NA, Beahrs TR, Politis CM, Sanders VM, Jones KJ. Exacerbation of facial motoneuron loss after facial nerve axotomy in CCR3-deficient mice. ASN Neuro. 2009b; 1(5):e00024.doi: 10.1042/AN20090017 [PubMed: 19922414]

Wainwright DA, Xin J, Mesnard NA, Politis CM, Sanders VM, Jones KJ. Effects of facial nerve axotomy on Th2- and Th1-associated chemokine expression in the facial motor nucleus of wild-type and presymptomatic mSOD1 mice. J Neuroimmunol. 2009c; 216(1-2):66–75. DOI: 10.1016/j.jneuroim.2009.09.009 [PubMed: 19818514]

Wajant H, Scheurich P. TNFR1-induced activation of the classical NF-kappaB pathway. FEBS J. 2011; 278(6):862–876. DOI: 10.1111/j.1742-4658.2011.08015.x [PubMed: 21232017]

Weber EM, Dallaire JA, Gaskill BN, Pritchett-Corning KR, Garner JP. Aggression in group-housed laboratory mice: why can't we solve the problem? Lab Anim (NY). 2017; 46(4):157–161. DOI: 10.1038/laban.1219 [PubMed: 28328884]

Werdelin L, Boysen G, Jensen TS, Mogensen P. Immunosuppressive treatment of patients with amyotrophic lateral sclerosis. Acta Neurol Scand. 1990; 82(2):132–134. [PubMed: 2256442]

Zamanian JL, Xu L, Foo LC, Nouri N, Zhou L, Giffard RG, Barres BA. Genomic analysis of reactive astrogliosis. J Neurosci. 2012; 32(18):6391–6410. DOI: 10.1523/JNEUROSCI.6221-11.2012 [PubMed: 22553043]

Highlights

- Immunodeficient mice have a suppressed glial response after facial nerve axotomy
- Neuroprotective WT CD4+ T cells regulate the glial microenvironment
- Intrinsic motoneuron regeneration response is independent of immune status
- mSOD1 whole splenocytes induce cell death pathways after axotomy
- New role proposed for the immune system in neurodegenerative diseases

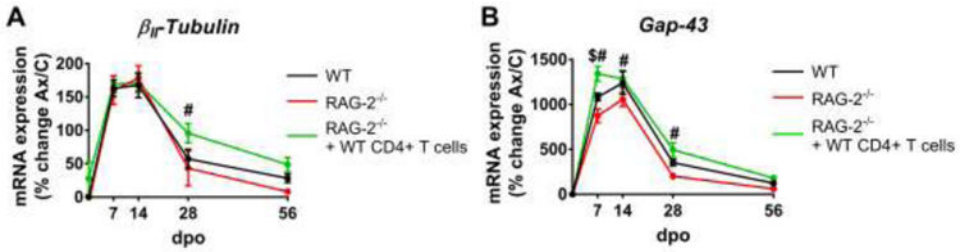

Figure 1.

mRNA expression of motoneuron regeneration-associated genes in the facial motor nucleus following facial nerve axotomy (Ax), relative to the control (C) facial motor nucleus. Mean percent change ± SEM was plotted across unoperated (0) and 7, 14, 28, and 56 days post operative (dpo) timepoints. Symbols used: $: $p < 0.05$ comparing WT to RAG-$2^{-/-}$ + WT CD4+ T cells and #: $p < 0.05$ comparing RAG-$2^{-/-}$ to RAG-$2^{-/-}$ + WT CD4+ T cells.

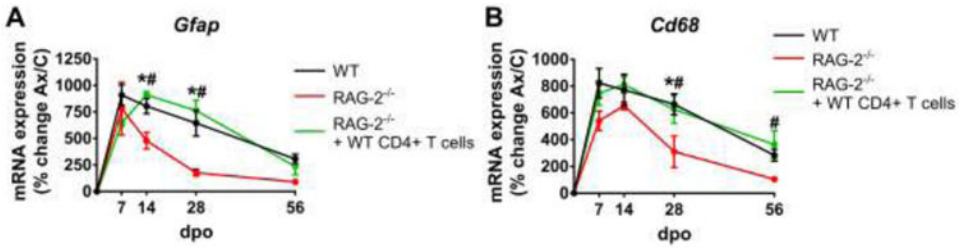

Figure 2.

mRNA expression of glial activation-associated genes comparing the axotomized (Ax) to the control (C) facial motor nucleus. Mean percent change ± SEM was plotted across uninjured (0) and 7, 14, 28, and 56 days post-operative (dpo) timepoints. Symbols used: *: $p < 0.05$ comparing WT to RAG-$2^{-/-}$ and #: $p < 0.05$ comparing RAG-2- - to RAG-$2^{-/-}$ + WT CD4+ T cells.

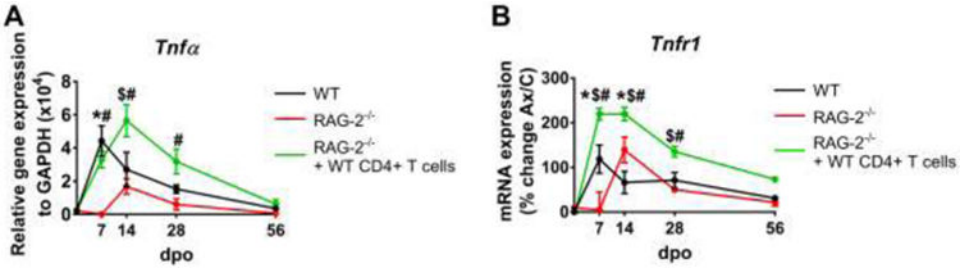

Figure 3.

Mean relative gene expression ± SEM of *Tnfα* compared to *Gapdh* in the axotomized facial motor nucleus (A). mRNA expression of *Tnfr1* comparing the axotomized (Ax) to the control (C) facial motor nucleus. Mean percent change ± SEM was plotted across uninjured (0) and 7, 14, 28, and 56 days post-operative (dpo) timepoints (B). Symbols used: *: $p < 0.05$ comparing WT to RAG-$2^{-/-}$; $: $p < 0.05$ comparing WT to RAG-$2^{-/-}$ + WT CD4+ T cells; and #: $p < 0.05$ comparing RAG-$2^{-/-}$ to RAG-$2^{-/-}$ + WT CD4+ T cells.

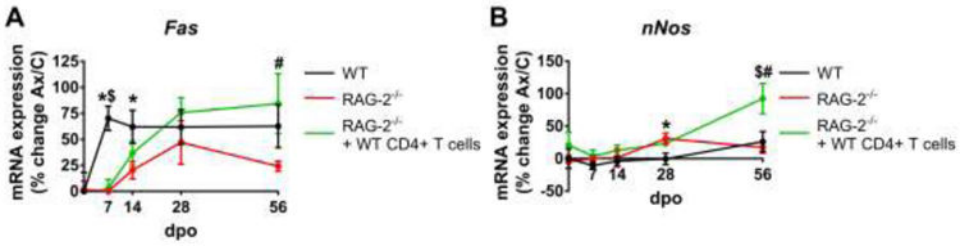

Figure 4.

mRNA expression of cell death-associated genes comparing the axotomized (Ax) to the control (C) facial motor nucleus. Mean percent change ± SEM was plotted across uninjured (0) and 7, 14, 28, and 56 days post-operative (dpo) timepoints. Symbols used: *: $p < 0.05$ comparing WT to RAG-$2^{-/-}$; $: $p < 0.05$ comparing WT to RAG-$2^{-/-}$ + WT CD4+ T cells; and #: $p < 0.05$ comparing RAG-$2^{-/-}$ to RAG-$2^{-/-}$ + WT CD4+ T cells.

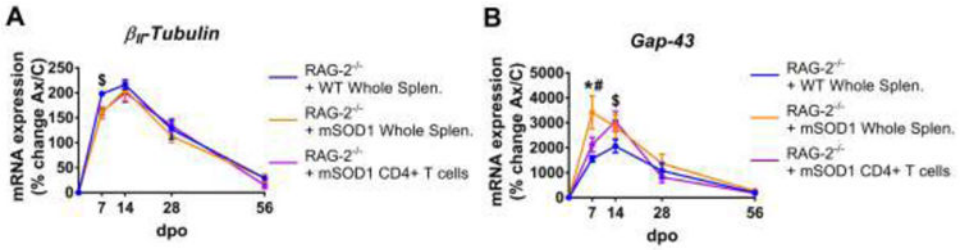

Figure 5.

mRNA expression of motoneuron regeneration-associated genes in the facial motor nucleus following facial nerve axotomy (Ax), relative to the control (C) facial motor nucleus. Mean percent change ± SEM was plotted across unoperated (0) and 7, 14, 28, and 56 days post operative (dpo) timepoints. Symbols used: *: $p < 0.05$ comparing RAG-$2^{-/-}$ + WT whole splenocytes to RAG-$2^{-/-}$ + mSOD1 whole splenocytes; $: $p < 0.05$ comparing RAG-$2^{-/-}$ + WT whole splenocytes to RAG-$2^{-/-}$ + mSOD1 CD4+ T cells; and #: $p < 0.05$ comparing RAG-$2^{-/-}$ + mSOD1 whole splenocytes to RAG-$2^{-/-}$ + mSOD1 CD4+ T cells.

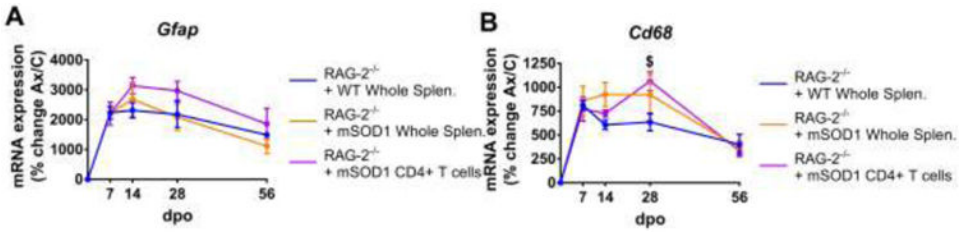

Figure 6.

mRNA expression of glial-associated genes in the facial motor nucleus following facial nerve axotomy (Ax), relative to the control (C) facial motor nucleus. Mean percent change ± SEM was plotted across unoperated (0) and 7, 14, 28, and 56 days post operative (dpo) timepoints. Symbols used: $: $p < 0.05$ comparing RAG-$2^{-/-}$ + WT whole splenocytes to RAG-$2^{-/-}$ + mSOD1 CD4+ T cells.

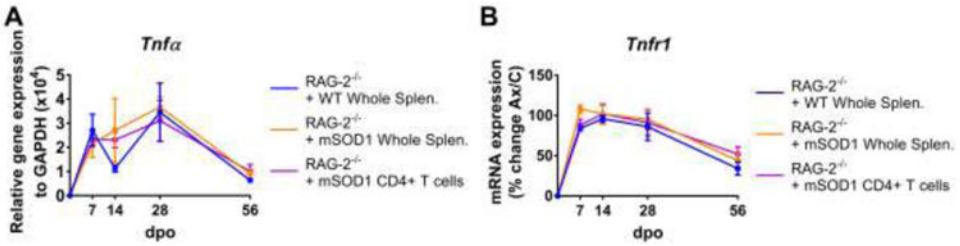

Figure 7.

Mean relative gene expression ± SEM of *Tnfα* compared to *Gapdh* in the axotomized facial motor nucleus (A). mRNA expression of *Tnfr1* comparing the axotomized (Ax) to the control (C) facial motor nucleus. Mean percent change ± SEM was plotted across uninjured (0) and 7, 14, 28, and 56 days post-operative (dpo) timepoints (B).

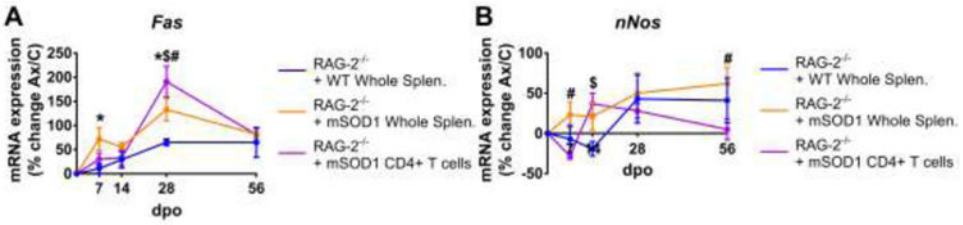

Figure 8.

mRNA expression of Fas/nNos cell death-associated genes in the facial motor nucleus following facial nerve axotomy (Ax), relative to the control (C) facial motor nucleus. Mean percent change ± SEM was plotted across unoperated (0) and 7, 14, 28, and 56 days post operative (dpo) timepoints. Symbols used: *: $p < 0.05$ comparing RAG-$2^{-/-}$ + WT whole splenocytes to RAG-$2^{-/-}$ + mSOD1 whole splenocytes; $: $p < 0.05$ comparing RAG-$2^{-/-}$ + WT whole splenocytes to RAG-$2^{-/-}$ + mSOD1 CD4+ T cells; and #: $p < 0.05$ comparing RAG-$2^{-/-}$ + mSOD1 whole splenocytes to RAG-$2^{-/-}$ + mSOD1 CD4+ T cells.

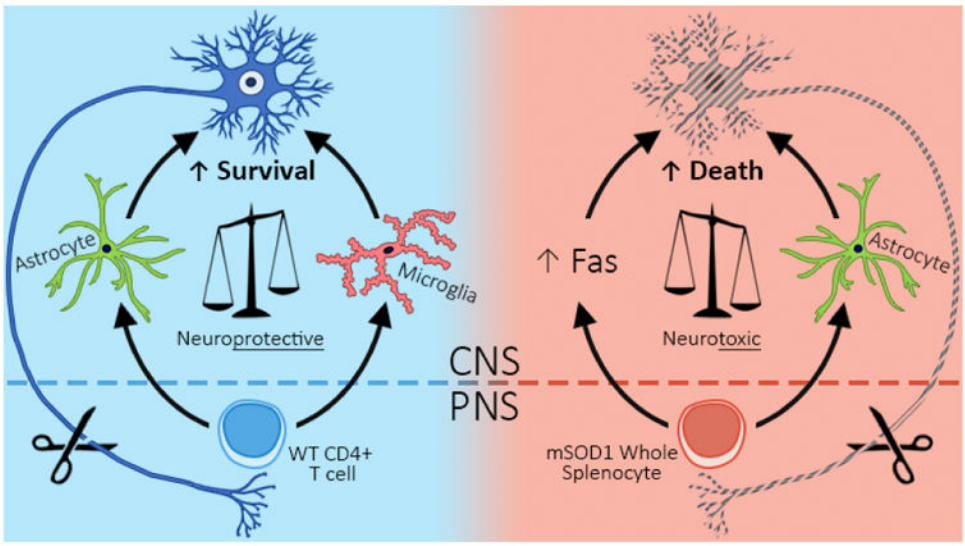

Figure 9.

Summary of findings from this study. On the left, WT CD4+ T cells are depicted as regulators of glial responses to axotomy, resulting in a neuroprotective glial microenvironment that promotes motoneuron survival. On the right, mSOD1 whole splenocytes are shown as generating a neurotoxic glial environment by promoting an aberrant astrocyte phenotype and increasing Fas expression, thereby contributing to greater motoneuron death.

Table 1

Catalog information for qPCR TaqMan assays ordered from Thermo Fisher Scientific.

Gene	TaqMan ID	RefSeq Accession Number
β_{II}-tubulin (Tubb2a)	Mm00809562_s1	NM_009450.2
Fas	Mm01204974_m1	NM_007987.2
Gap-43	Mm01144975_m1	NM_008083.2
Gapdh	Mm99999915_g1	NM_001289726.1, NM_008084.3
Gfap	Mm01253033_m1	NM_001131020.1, NM_010277.3
nNos (Nos1)	Mm00435175_m1	D14552.1 (GenBank)
Tnfα	Mm00443260_g1	NM_013693.3